



UvA-DARE (Digital Academic Repository)

Discovery of water vapour in the carbon star V Cygni from observations with Herschel/HIFI

Neufeld, D.A.; González-Alfonso, E.; Melnick, G.; Puecka, M.; Schmidt, M.; Szczerba, R.; Bujarrabal, V.; Alcolea, J.; Cernicharo, J.; Decin, L.K.E.; Dominik, C.; Justanont, K.; de Koter, A.; Marston, A.P.; Menten, K.; Olofsson, H.; Planesas, P.; Schöier, F.L.; Teyssier, D.; Waters, L.B.F.M.; Edwards, K.; McCoey, C.; Shipman, R.; Jellema, W.; de Graauw, T.; Ossenkopf, V.; Schieder, R.; Philipp, S.

Published in:
Astronomy & Astrophysics

DOI:
[10.1051/0004-6361/201015080](https://doi.org/10.1051/0004-6361/201015080)

[Link to publication](#)

Citation for published version (APA):

Neufeld, D. A., González-Alfonso, E., Melnick, G., Puecka, M., Schmidt, M., Szczerba, R., ... Philipp, S. (2010). Discovery of water vapour in the carbon star V Cygni from observations with Herschel/HIFI. *Astronomy & Astrophysics*, 521, L5. DOI: 10.1051/0004-6361/201015080

General rights

It is not permitted to download or to forward/distribute the text or part of it without the consent of the author(s) and/or copyright holder(s), other than for strictly personal, individual use, unless the work is under an open content license (like Creative Commons).

Disclaimer/Complaints regulations

If you believe that digital publication of certain material infringes any of your rights or (privacy) interests, please let the Library know, stating your reasons. In case of a legitimate complaint, the Library will make the material inaccessible and/or remove it from the website. Please Ask the Library: <http://uba.uva.nl/en/contact>, or a letter to: Library of the University of Amsterdam, Secretariat, Singel 425, 1012 WP Amsterdam, The Netherlands. You will be contacted as soon as possible.

LETTER TO THE EDITOR

Discovery of water vapour in the carbon star V Cygni from observations with *Herschel*/HIFI[★]

D. A. Neufeld¹, E. González-Alfonso², G. Melnick³, M. Pućecka⁴, M. Schmidt⁴, R. Szczerba⁴, V. Bujarrabal⁵, J. Alcolea⁶, J. Cernicharo⁷, L. Decin^{8,9}, C. Dominik^{9,15}, K. Justtanont¹⁰, A. de Koter^{9,16}, A. P. Marston¹¹, K. Menten¹², H. Olofsson^{10,13}, P. Planesas^{5,14}, F. L. Schöier¹⁰, D. Teyssier¹¹, L. B. F. M. Waters^{9,8}, K. Edwards¹⁷, C. McCoey¹⁷, R. Shipman¹⁸, W. Jellema¹⁸, T. de Graauw¹⁹, V. Ossenkopf²⁰, R. Schieder²⁰, and S. Philipp¹²

¹ The Johns Hopkins University, 3400 North Charles St, Baltimore, MD 21218, USA
e-mail: neufeld@pha.jhu.edu

² Departamento de Física, Universidad de Alcalá de Henares, Campus Universitario, 28871 Alcalá de Henares, Madrid, Spain

³ Harvard-Smithsonian Center for Astrophysics, Cambridge, MA 02138, USA

⁴ N. Copernicus Astronomical Center, Rabiańska 8, 87-100 Toruń, Poland

⁵ Observatorio Astronómico Nacional (IGN), Ap 112, 28803 Alcalá de Henares, Spain

⁶ Observatorio Astronómico Nacional (IGN), Alfonso XII No. 3, 28014 Madrid, Spain

⁷ CAB, INTA-CSIC, Ctra de Torrejón a Ajalvir, km 4, 28850 Torrejón de Ardoz, Madrid, Spain

⁸ Instituut voor Sterrenkunde, Katholieke Universiteit Leuven, Celestijnenlaan 200D, 3001 Leuven, Belgium

⁹ Sterrenkundig Instituut Anton Pannekoek, University of Amsterdam, Science Park 904, 1098 Amsterdam, The Netherlands

¹⁰ Onsala Space Observatory, Dept. of Radio and Space Science, Chalmers University of Technology, 43992 Onsala, Sweden

¹¹ European Space Astronomy Centre, ESA, PO Box 78, 28691 Villanueva de la Cañada, Madrid, Spain

¹² Max-Planck-Institut für Radioastronomie, Auf dem Hügel 69, 53121 Bonn, Germany

¹³ Department of Astronomy, AlbaNova University Center, Stockholm University, 10691 Stockholm, Sweden

¹⁴ Joint ALMA Observatory, El Golf 40, Las Condes, Santiago, Chile

¹⁵ Department of Astrophysics/IMAPP, Radboud University Nijmegen, Nijmegen, The Netherlands

¹⁶ Astronomical Institute, Utrecht University, Princetonplein 5, 3584 CC Utrecht, The Netherlands

¹⁷ University of Waterloo, and University of Western Ontario, Canada

¹⁸ SRON Netherlands Institute for Space Research, Landleven 12, 9747 AD Groningen, The Netherlands

¹⁹ Atacama Large Millimeter/Submillimeter Array, Joint ALMA Office, Santiago, Chile

²⁰ KOSMA, I. Physik. Institut, Universität zu Köln, Zùlpicher Str. 77, 50937 Köln, Germany

Received 28 May 2010 / Accepted 6 July 2010

ABSTRACT

We report the discovery of water vapour toward the carbon star V Cygni. We have used *Herschel*'s HIFI instrument, in dual beam switch mode, to observe the $1_{11}-0_{00}$ para-water transition at 1113.3430 GHz in the upper sideband of the Band 4b receiver. The observed spectral line profile is nearly parabolic, but with a slight asymmetry associated with blueshifted absorption, and the integrated antenna temperature is 1.69 ± 0.17 K km s⁻¹. This detection of thermal water vapour emission, carried out as part of a small survey of water in carbon-rich stars, is only the second such detection toward a carbon-rich AGB star, the first having been obtained by the *Submillimeter Wave Astronomy Satellite* toward IRC+10216. For an assumed ortho-to-para ratio of 3 for water, the observed line intensity implies a water outflow rate $\sim 3-6 \times 10^{-5}$ Earth masses per year and a water abundance relative to H₂ of $\sim 2-5 \times 10^{-6}$. This value is a factor of at least 10⁴ larger than the expected photospheric abundance in a carbon-rich environment, and – as in IRC+10216 – raises the intriguing *possibility* that the observed water is produced by the vapourisation of orbiting comets or dwarf planets. However, observations of the single line observed to date do not permit us to place strong constraints upon the spatial distribution or origin of the observed water, but future observations of additional transitions will allow us to determine the inner radius of the H₂O-emitting zone, and the H₂O ortho-to-para ratio, and thereby to place important constraints upon the origin of the observed water emission.

Key words. stars: AGB and post-AGB – circumstellar matter – submillimeter: stars

1. Introduction

The carbon-to-oxygen ratio is the critical determinant of the photospheric chemistry in evolved stars; the photospheres of oxygen rich-stars, with C/O ratios < 1, are dominated by CO and H₂O, while those of carbon-rich stars are dominated by CO, HCN, and C₂H₂ and contain very little H₂O. Despite this

sharp dichotomy in photospheric composition, water vapour has previously been discovered, using the Submillimeter Wave Astronomy Satellite (SWAS), in the circumstellar outflow of the extreme carbon star IRC+10216 (Melnick et al. 2001), for which the C/O ratio is ~ 1.4 . The observation of water vapour in that source, with an inferred abundance relative to H₂ of $\sim 10^{-7}$ (Agúndez & Cernicharo 2006; González-Alfonso et al. 2007), has led to the suggestion of several possible origins for the water vapour, including (1) the vapourisation of icy objects (comets or dwarf planets) in orbit around the star (Ford & Neufeld 2001);

[★] *Herschel* is an ESA space observatory with science instruments provided by European-led Principal Investigator consortia and with important participation from NASA.

(2) Fischer-Tropsch catalysis (Willacy 2004); (3) photochemistry within an outer, photodissociated shell (Agúndez & Cernicharo 2006); (4) photochemistry within a clumpy outflow (Decin et al. 2010). In both carbon- and oxygen-rich stars, Cherchneff (2006) and Decin et al. (2008) have argued for the importance of shocks in setting non-equilibrium abundances of the molecules CO, HCN, CS, and SiO within the inner envelope, although existing models do not appear to predict a persistent enhancement of H₂O in stars with C/O > 1.

Using the HIFI instrument (de Graauw et al. 2010) on *Herschel* (Pilbratt et al. 2010), it is now possible to search with unprecedented sensitivity for water vapour in carbon-rich stars. As part of the HIFISTARS guaranteed time key program, we will carry out a survey for water vapour in eight carbon-rich stars at distances greater than that (~170 pc) of IRC+10216. Here, we report the detection of water vapour in the very first carbon star targeted in this survey: V Cygni, a Mira variable of spectral type C6 (Wallerstein & Knapp 1998), with an apparent *V* magnitude varying from 13.9 to 7.7 mag, a period of 421 days, and a distance of ~400 pc (Biegging & Wilson 2001).

2. Observations and results

We observed the lowest transition of para-water, the 1₁₁-0₀₀ transition at 1113.3430 GHz line, in the upper sideband of the Band 4b HIFI receiver. This observation, of duration 1167 s including overheads, was carried out on 2010 March 5, using the dual beam switch (DBS) mode and the wide band spectrometer (WBS). The WBS has a spectral resolution of 1.1 MHz, corresponding to a velocity resolution of 0.30 km s⁻¹ at the frequency of the 1₁₁-0₀₀ transition. The telescope beam, of half-power-beam-width (HPBW) ~ 20'', was centered on V Cygni at coordinates $\alpha = 20\text{h}41\text{m}18.3\text{s}$, $\delta = 48^\circ08'29''$ (J2000). The reference positions for this observation were located at offsets of 3' on either side of the source.

The data were processed using the standard HIFI pipeline to Level 2, providing fully calibrated spectra of the source. The Level 2 data were analysed further using the *Herschel* interactive processing environment (HIPE; Ott 2010), version 2.4, along with ancillary IDL routines that we have developed. Having found the signals measured in the two orthogonal polarizations to be in excellent agreement, we combined them to obtain an average spectrum. Figure 1 shows the WBS spectrum of para-H₂O 1₁₁-0₀₀ obtained toward V Cygni, with the frequency scale expressed as Doppler velocities relative to the Local Standard of Rest (LSR) and the intensity scale expressed as antenna temperature. A zeroth-order baseline has been subtracted. The vertical dashed line indicates the LSR velocity of the source, as determined by Biegging & Wilson (2001, hereafter BW01) from observations of the CO *J* = 2-1 line. The integrated antenna temperature is found to be 1.69 ± 0.17 K km s⁻¹. Our identification of the observed feature with the para-H₂O 1₁₁-0₀₀ transition is supported by the absence of any plausible alternative candidate in the JPL (Pickett et al. 1998) or CDMS (Müller et al. 2001) spectral line catalogues.

3. Derivation of the water outflow rate and abundance

In modeling the water emission from V Cygni, we have used the methods described by González-Alfonso et al. (2007, hereafter GNM). To determine the H₂O rotational populations and

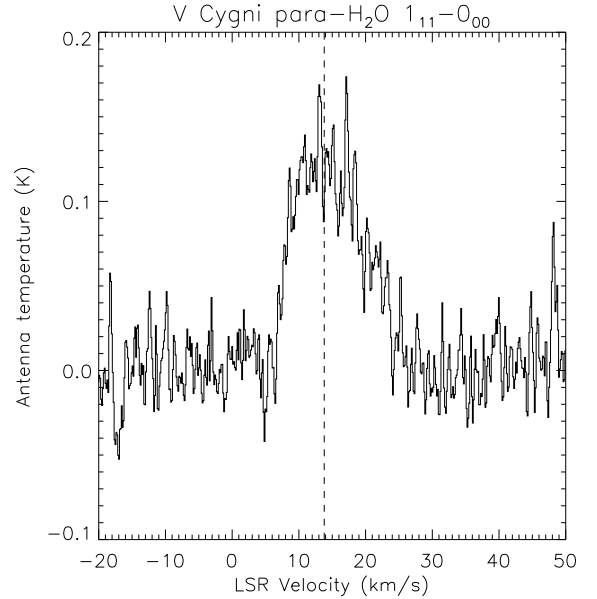


Fig. 1. Continuum-subtracted spectrum of para-H₂O 1₁₁-0₀₀ obtained toward V Cygni. The vertical dashed line indicates the LSR velocity of the source, as determined by BW01 from observations of the CO *J* = 2-1 line.

Table 1. Assumed parameters for V Cygni.

Distance: 400 pc
Stellar luminosity: 8500 L_{\odot}
Effective temperature: 2500 K
Stellar radius: 3.42×10^{13} cm
Systemic LSR velocity: +13.8 km s ⁻¹
Terminal outflow velocity: 11.8 km s ⁻¹

the resultant H₂O emission spectrum, we included the effects of radiative pumping – through the $\nu_2 = 1$ and $\nu_3 = 1$ vibrational states – and of collisional excitation by H₂, together with a treatment of radiative transfer based upon that discussed by González-Alfonso & Cernicharo (1997).

The assumed parameters for the source are summarized in Table 1 and discussed below. A variety of distance estimates for V Cygni have appeared in the literature. BW01 obtained values of 406 pc and 456 pc respectively by using the *P* – *K* (period – absolute *K* magnitude) and *P* – *L* (period – bolometric luminosity) relationships presented by Groenewegen & Whitelock (1996, hereafter GW96). However, our own fit to the spectral energy distribution (SED), shown in Fig. 2, implies that a distance of 342 pc is required to fit the GW96 *P* – *L* relationship. Here, we used a dust radiative transfer model to fit a combination of flux measurements from *Tycho*, *Hipparcos*, *MSX*, *2MASS*, *ISO*, *IRAS*, and *JCMT*. This model, full details of which will be presented in a future publication (Schmidt et al., in prep.), assumes a power-law distribution of grain radii with index –3.5 between 0.005 and 0.25 μm , a maximum dust temperature of 1050 K, an inner radius for the dust shell of 2×10^{14} cm, and a total optical depth $A_V = 9.45$ mag. A smaller distance estimate (370 pc) than those of BW01 was also obtained by Schöier & Olofsson (2000). All of the values mentioned above are consistent with the *Hipparcos*-measured parallax of 3.69 ± 1.77 mas, which implies a 1σ distance range of 180–520 pc. Accordingly, we adopt a value of 400 pc for the estimated distance of V Cygni, with a likely uncertainty ~20%.

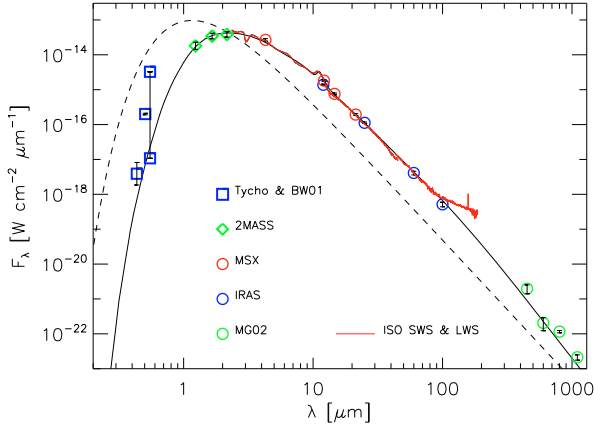


Fig. 2. Spectral energy distribution of V Cygni. A dust radiative transfer model (see text) has been used to fit the fluxes measured by *Tycho*, *MSX*, *2MASS*, *ISO*, *IRAS*, and *JCMT*. The dashed curve shows the unattenuated photospheric emission, while the solid curve shows the total emission from the attenuated photosphere and surrounding dust.

This estimate of the distance then requires a bolometric luminosity of $8500 L_{\odot}$ to match the observed SED shown in Fig. 2, and a stellar radius of 3.42×10^{13} cm, given an assumed effective temperature of 2500 K. The values given in Table 1 for the systemic velocity of the source and the terminal velocity of the outflow were based upon *Herschel*/HIFI observations of the CO $J = 6-5$ transition at 691.473 GHz (Schmidt et al., in prep.) and are in excellent agreement with previous determinations by BW01. To obtain an estimate of the total mass-loss rate in the outflow, we have modeled the fluxes observed by *Herschel*/HIFI for the CO $J = 6-5$, $J = 10-9$ and $J = 16-15$ transitions. Full details of the observations and modeling of CO will be given by Schmidt et al., in prep.). Our best estimate of the gas mass-loss rate in the inner envelope is $4.6 \times 10^{-6} M_{\odot} \text{ yr}^{-1}$, a factor ~ 3 larger than that obtained by Schöier & Olofsson (2000) from a fit to the CO $J = 2-1$ transition, and the derived CO/H₂ ratio is 10^{-3} . Indeed, we find that a constant mass-loss rate model that fits the CO $J = 6-5$, $J = 10-9$ and $J = 16-15$ transitions substantially overpredicts the flux in the CO $J = 2-1$ transition. This discrepancy suggests some variability in the mass-loss rate, with a larger value applying to the inner envelope where the higher-lying transitions of CO originate. We obtained a satisfactory fit to both the CO rotational line fluxes and the continuum spectrum by assuming a gas and dust density that decreases as radius^{-2.15}, instead of the radius⁻² density profile expected for an envelope with a constant mass loss rate and outflow velocity. The gas-to-dust mass ratio in this model is 510.

Fortunately, given the significant uncertainties in many of the assumed parameters listed in Table 1, the derived water outflow rate is not strongly dependent upon any of them. As discussed in GNM, unless the mass-loss rate is extremely large, the excitation of water is dominated by radiative pumping via the $6 \mu\text{m}$ ν_2 band. Thus, for a given water outflow rate, the observed water line fluxes scale linearly with the observed $6 \mu\text{m}$ continuum flux. Since the latter is an observed (rather than a derived) quantity, our estimate of the water outflow rate is largely independent of the distance or total outflow rate assumed for the source.

In modeling the water line strength and profile observed toward V Cygni, we have investigated two models for the spatial distribution of the observed water. In Model A, we assume that water is present at radii as small as 4.5×10^{14} cm, while in Model B, we adopt an inner radius $R_{\text{in}} = 2 \times 10^{15}$ cm at which the water is injected into the outflow. In both cases, we assume

Table 2. Derived parameters for V Cygni.

Model A: Water inner radius = 4.5×10^{14} cm
Para-water abundance relative to H ₂ : 5.3×10^{-7}
Total water abundance ^a relative to H ₂ : 2.1×10^{-6}
Total water outflow rate: 3×10^{-5} Earth mass/yr
Model B: Water inner radius = 2×10^{15} cm
Para-water abundance relative to H ₂ : 1.0×10^{-6}
Total water abundance ^a relative to H ₂ : 4.2×10^{-6}
Total water outflow rate: 6×10^{-5} Earth mass/yr

Notes. ^(a) For an assumed ortho-to-para ratio of 3.

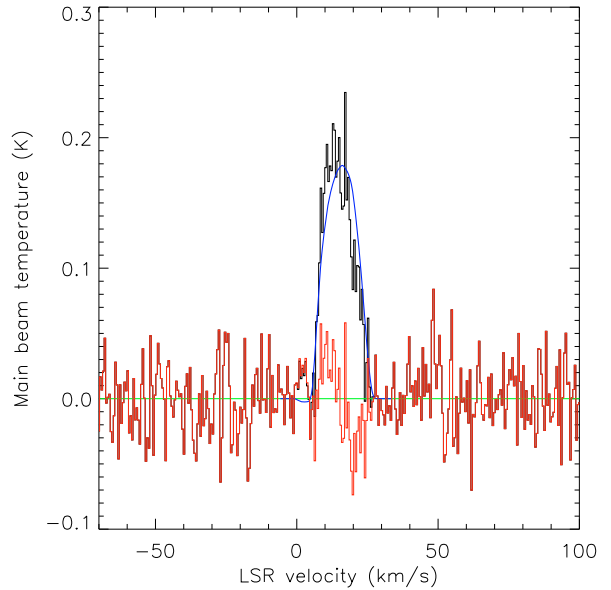


Fig. 3. Continuum-subtracted and smoothed spectrum of the $1_{11}-0_{00}$ transition of para-water at 1113.3430 GHz (black), compared with the best fit from Model B (blue). The residuals are shown in red. Here, the vertical axis is the main beam brightness temperature, obtained by dividing the antenna temperature by an assumed main beam efficiency of 0.67.

an outer radius of $R_{\text{out}} = 1 \times 10^{16}$ cm, the estimated photodissociation radius for water¹.

The distribution assumed in Model B is expected if the vapourisation of icy objects is the origin of the observed water vapour, since all such objects at smaller distances from the star will have been vapourised already (Ford & Neufeld 2001, GNM). In both models, we adopted the profile given by Goldreich & Scoville (1976) for the outflow velocity as a function of radius. For Model B, this velocity profile was found to give a better fit to the observed line shape than an alternative velocity profile, based upon the work of Skinner et al. (1999), which entails a more rapid acceleration of the outflowing material. A clear asymmetry in the line profile, apparently associated

¹ The mean lifetime against photodissociation for a water molecule in the unshielded mean Galactic ultraviolet radiation field is 1.2×10^9 s (Roberge et al. 1991), corresponding to a distance of 1.4×10^{15} cm at the terminal outflow velocity of the V Cygni outflow. Shielding by dust in the outflow increases this distance by a factor of several, leading to photodissociation radii ranging from $\sim 5-10 \times 10^{15}$ cm² for radiation fields within a factor of two of the mean Galactic value. We adopt the upper end of this range, in order to obtain a conservative estimate of the water outflow rate. To account for the observed water line strength, smaller values of R_{out} would require larger values of the water abundance.

with blueshifted absorption, suggests a significant turbulent velocity width, of order 1.3 km s^{-1} . *Equally good fits can be obtained for models A and B, implying that our current observations (of a single line) cannot be used to provide useful constraints on the spatial distribution or origin of the water vapour in V Cygni.* The best-fit parameters are given in Table 2, for each of the two models, and the fit for Model B is shown in Fig. 3. For an assumed water ortho-to-para ratio of 3, the required water outflow rates are 3×10^{-5} and 6×10^{-5} Earth masses per year for models A and B respectively.

4. Discussion

Our detection of thermal water vapour from V Cygni is only the second such detection from the circumstellar envelope of a carbon-rich AGB star, the first having been obtained toward IRC+10216. The water outflow rate in V Cygni, $3\text{--}6 \times 10^{-5}$ Earth masses per year, is 4–8 times that in IRC+10216, even though the total mass outflow rate of $4.6 \times 10^{-6} M_{\odot} \text{ yr}^{-1}$ is smaller by a factor ~ 8 . Thus the water line luminosity in V Cygni implies a water abundance $\sim 30\text{--}60$ times as large as that inferred for IRC+10216. The large H_2O abundance $\sim 3\text{--}6 \times 10^{-6}$ that we infer is at least a factor of 10^4 larger than that predicted in models for the photospheres of C-rich stars in thermochemical equilibrium (e.g. Cherchneff 2006). As in IRC+10216, the inferred abundance raises the intriguing *possibility* that the water is produced by the vapourisation of orbiting comets or dwarf planets. In this picture (Ford & Neufeld 2001), a collection of orbiting icy objects in a Kuiper-belt analogue are vapourised as the star ascends the asymptotic giant branch and its luminosity gradually increases; to match the observed water outflow rate in V Cygni, this scenario would require a reservoir of ~ 10 Earth masses of water ice available for release during the AGB phase.

Observations of the single water line observed to date, however, do not permit us to place strong constraints upon the spatial distribution or origin of the observed water, but future observations of additional transitions will allow us to determine the inner radius, R_{in} , of the H_2O -emitting zone, as well as the H_2O ortho-to-para ratio. The radius, R_{in} , is a critical diagnostic, because the comet vapourisation model predicts a value $\sim 2 \times 10^{15} \text{ cm}$ (Model B), all orbiting icy objects within that radius having already been vapourised. In Table 3, we present predictions for the strengths of various emission lines lying within the spectral range accessible to the HIFI, SPIRE and PACS instruments on *Herschel*. In the HIFI (and SPIRE) spectral range (upper section of Table 3), results are given as integrated antenna temperatures; in the PACS spectral range (lower section), the values given are fluxes, in units $10^{-16} \text{ W m}^{-2}$. The predictions presented here are for an assumed ortho-to-para ratio of 3. Several lines, such as the $916.171 \text{ GHz } 4_{22}\text{--}3_{31}$ transition observable by HIFI and the $6_{16}\text{--}5_{05} 82.031 \mu\text{m}$ transition observable by PACS, show a strong dependence upon R_{in} and should provide an excellent discriminant between different models.

Acknowledgements. HIFI has been designed and built by a consortium of institutes and university departments from across Europe, Canada and the United States under the leadership of SRON Netherlands Institute for Space Research, Groningen, The Netherlands and with major contributions from Germany, France and the US. Consortium members are: Canada: CSA, U. Waterloo; France: CESR, LAB, LERMA, IRAM; Germany: KOSMA, MPIfR, MPS; Ireland, NUI Maynooth; Italy: ASI, IFSI-INAF, Osservatorio Astrofisico di Arcetri-INAF; The Netherlands: SRON, TUD; Poland: CAMK, CBK; Spain: Observatorio Astronómico Nacional (IGN), Centro de Astrobiología (CSIC-INTA). Sweden: Chalmers University of Technology – MC2, RSS & GARD; Onsala Space Observatory; Swedish National Space Board, Stockholm University – Stockholm Observatory; Switzerland: ETH Zurich, FHNW;

Table 3. Predicted line strengths for V Cygni.

Transition	Frequency (GHz)	Wavelength (μm)	Line strength $\int T_{\text{MB}} dv$ in $\text{K km s}^{-1} a$	
			Model A	Model B
$1_{11}\text{--}0_{00}$	1113.343	269.272	2.53 ^a	2.53 ^b
$2_{02}\text{--}1_{11}$	987.927	303.456	2.46	2.79
$2_{11}\text{--}2_{02}$	752.033	398.643	1.18	1.17
$2_{20}\text{--}2_{11}$	1228.789	243.974	0.56	0.56
$4_{22}\text{--}3_{31}$	916.171	327.223	0.47	0.02
$1_{10}\text{--}1_{01}$	556.936	538.289	1.16	1.06
$2_{12}\text{--}1_{01}$	1669.905	179.527	6.40	5.90
$2_{21}\text{--}2_{12}$	1661.008	180.488	1.92	1.79
$3_{03}\text{--}2_{12}$	1716.770	174.626	5.43	4.93
$3_{12}\text{--}2_{21}$	1153.126	259.982	1.37	0.85
$3_{12}\text{--}3_{03}$	1097.365	273.193	1.67	1.49
$3_{21}\text{--}3_{12}$	1162.911	257.795	0.65	0.59
$4_{32}\text{--}5_{05}$	1713.882	174.920	0.64	0.03
Transition	Frequency (GHz)	Wavelength (μm)	Line strength ($10^{-16} \text{ W m}^{-2}$)	
			Model A	Model B
$2_{11}\text{--}2_{02}$	2968.748	100.983	1.27	0.82
$3_{31}\text{--}2_{20}$	4468.572	67.089	1.16	0.42
$2_{21}\text{--}1_{10}$	2773.976	108.073	2.20	1.67
$3_{21}\text{--}2_{12}$	3977.045	75.381	2.61	1.11
$4_{14}\text{--}3_{03}$	2640.473	113.537	1.70	0.70
$3_{30}\text{--}2_{21}$	4512.385	66.438	2.51	1.12
$4_{32}\text{--}3_{12}$	3807.256	78.742	1.72	0.23
$5_{05}\text{--}4_{14}$	3013.199	99.493	1.23	0.22
$4_{32}\text{--}3_{21}$	5107.284	58.699	1.73	0.35
$6_{16}\text{--}5_{05}$	3654.602	82.031	1.20	0.02

Notes. ^(a) Integrated main beam temperature; ^(b) observed line strength.

USA: Caltech, JPL, NHSC. This research was performed, in part, through a JPL contract funded by the National Aeronautics and Space Administration. R.Sz. and M.Sch. acknowledge support from grant N 203 393334 from Polish MNiSW. E.G.-A. is a Research Associate at the Harvard-Smithsonian Center for Astrophysics. This work has been partially supported by the Spanish MICINN, program CONSOLIDER INGENIO 2010, grant ASTROMOL (CSD2009-00038).

References

- Agúndez, M., & Cernicharo, J. 2006, *ApJ*, 650, 374
 Biegging, J. H., & Wilson, C. D. 2001, *AJ*, 122, 979
 Cherchneff, I. 2006, *A&A*, 456, 1001
 Decin, L., Cherchneff, I., Hony, S., et al. 2008, *A&A*, 480, 431
 Decin, L., Agúndez, M., Barlow, M. J., et al. 2010, *Nature*, 467, 64
 de Graauw, Th., Helmich, F. P., Phillips, T. G., et al. 2010, *A&A*, 518, L6
 Ford, K. E., & Neufeld, D. A. 2001, *ApJ*, 557, L113
 González-Alfonso, E., & Cernicharo, J. 1997, *A&A*, 322, 938
 González-Alfonso, E., Neufeld, D. A., & Melnick, G. J. 2007, *ApJ*, 669, 412
 Goldreich, P., & Scoville, N. 1976, *ApJ*, 205, 144
 Groenewegen, M. A. T., & Whitelock, P. A. 1996, *MNRAS*, 281, 1347
 Melnick, G. J., Neufeld, D. A., Ford, K. E. S., Hollenbach, D. J., & Ashby, M. L. N. 2001, *Nature*, 412, 160
 Müller, H. S. P., Thorwirth, S., Roth, D. A., & Winnewisser, G. 2001, *A&A*, 370, L49
 Ott, S. 2010, in *Astronomical Data Analysis Software and Systems XIX*, ed. Y. Mizumoto, K.-I. Morita, & M. Ohishi, ASP Conf. Ser., in press
 Pickett, H. M., Poynter, I. R. L., Cohen, E. A., et al. 1998, *J. Quant. Spectrosc. Radiat. Transf.*, 60, 883
 Pilbratt, G. L., Riedinger, J. R., Passvogel, T., et al. 2010, *A&A*, 518, L1
 Roberge, W. G., Jones, D., Lepp, S., & Dalgarno, A. 1991, *ApJS*, 77, 287
 Schöier, F. L., & Olofsson, H. 2000, *A&A*, 359, 586
 Skinner, C. J., Justtanont, K., Tielens, A. G. G. M., et al. 1999, *MNRAS*, 302, 293
 Wallerstein, G., & Knapp, G. R. 1998, *ARA&A*, 36, 369
 Willacy, K. 2004, *ApJ*, 600, L87